Regional Variability of Climate Change Hot-spots in Africa

U.M.Anber[1], M.M.AbdelWahab[1], D.Yates[2]

[1]Department of Astronomy and Meteorology,
Faculty of Science,
Cairo University,
Cairo, Egypt

[2]National Center for Atmospheric Research,Boulder,Colorado,U.S.A

Abstract

The Regional Climate Change Index (RCCI) is employed to investigate hot-spots under 21st century global warming over Africa. The RCCI is calculated on 1-degree resolution grid from the ensemble of CMIP3 simulations for the A1B, A2 and B1 IPCC emission scenarios. The RCCI over Africa captured sub-regional variability over the seven sub-regional hot-spots –such as Southern Mediterranean, Sahara, Western Africa, Eastern Africa, Equatorial Africa, Southern Equatorial Africa, and Southern Africa. Contributions from different factors to the RCCI are discussed for the sub-regions. Analysis of the temporal evolution of the hot-spots throughout the 21st century shows different rates of response time to global warming for the different sub-regions. Hot-spots have emerged in the Southern Mediterranean and Sahara. These hot-spots become evident by the mid of the 21st century and it is the most prominent by the end of the century. While hot-pots are generally evident in all the 7 sub-regions for the A2 scenario, in the A1B scenario, the hot-spots of Southern Mediterranean, Sahara, and South Africa emerge in the last 20 year period of the 21st century. No hot-spot emerge in the B1 scenario, which has the lowest GHG concentrations except for the Southern Mediterranean during the period 2061-2080. Our analysis indicates that sub-regional hot-spots show a rather complex spatial and temporal dependency on the GHG concentration and on the different factors contributing to the RCCI.

1. Introduction

Lying between latitudes 37° north and 35° south, Africa has virtually the same climatic zones in the Northern Hemisphere as in the Southern Hemisphere, and they are arranged symmetrically on either side of the equator. The zones are determined mainly by latitude, except in the east where highlands greatly modify the climate. Africa is the most tropical of the continents: Only its northern and southern extremes are directly influenced by mid-latitude westerly winds and are considered to have temperate climates.

Most of Africa lies between the Tropic of Cancer (in the north) and the Tropic of Capricorn (in the south) and has high temperatures throughout the year. The amount, duration, and seasonal distribution of rainfall is therefore the most important factor differentiating its climates. Africa

has six types of climatic zones: tropical wet, tropical summer rainfall, semiarid, arid, highland, and Mediterranean.

It is by now well established that greenhouse gas (GHG) emissions of anthropogenic origin have affected the Earth's climate in the 20th century and will increasingly do so in the 21st. As reported by IPCC (2007), the observed global average warming in the last hundred years (1906–2005) is about 0.74°C (0.56-0.92°C) and most of the warming since the mid-20th is very likely due to the increase in anthropogenic greenhouse gas concentrations. It is projected that global warming by the end of the 21st century (2090–2099) relative to 1980–1999 will be in the range of 1.1-6.0°C depending on the underlying GHG emission pathway.

This paper examining the change of African climate, especially temperature and rainfall, is set in the wider context of our emerging understanding of human influences on the larger, global-scale climate. Increasing greenhouse gas accumulation in the global atmosphere and increasing regional concentrations of aerosol particulates are now understood to have detectable effects on the global climate system (Santer et al. 1996). These effects will be manifest at regional scales although perhaps in more uncertain terms (Mitchell & Hulme 1999, Giorgi & Francisco 2000). Africa will not be exempt from experiencing these human-induced changes in climate.

Nevertheless, it is of considerable interest to try and explore the magnitude of the problem that the enhanced greenhouse effect may pose for African climate and for African resource managers. The sensitivity of the climate response to global warming over different regions is a critical issue in current international climate change research because this information is needed for impact assessment and adaptation policies. In a previous paper, Giorgi (2006) developed a Regional Climate Change Index (RCCI) to identify the relative response of different regions of the world to GHG-induced global warming. The RCCI is based on the change in mean and interannual variability of temperature and precipitation averaged over a given area and it measures the relative response to global warming across regions. Giorgi (2006) calculated the RCCI for 26 land regions of sub-continental size from the Phase 3 of the Coupled Model Intercomparison Project (CMIP3) ensemble of simulations recently conducted with coupled Atmosphere-Ocean General Circulation Models (AOGCMs) in support of the fourth assessment report of the Intergovernmental Panel on Climate Change (IPCC AR4). Giorgi (2006) identified a number of prominent climate change hot-spots, in particular the Mediterranean, Northeastern Europe and Central America.

It is important to stress that, as will be seen, the RCCI is a comparative index, that is a small RCCI value does not imply a small absolute change, but only a small climate response compared to other regions, which means that we can consider the RCCI as a sensitivity index.

In this chapter we will present the result of our analysis over seven regions in Africa and determine the regions that will exhibit big, moderate and small climate response under three scenarios A1B, A2 and B1 i.e. over their average "Ensemble".

Therefore in this paper we perform a RCCI analysis along the lines of that introduced by Giorgi (2006) but at a higher horizontal resolution over Africa. This allows us to quantify the sub-regional variability of the climate response to global warming and to identify whether climate

change hot-spots exist over different sub-regions of Africa. The analysis is performed using the same definition of RCCI as in Giorgi (2006) and the same set of AOGCM simulations. We also address issues of sensitivity of the RCCI to different GHG emission scenarios and to different periods within the 21st century.

We will, also, follow the RCCI in the five 20-year periods of the 21st century to study the dependency of the regional hot-spots on the GHG forcing, under A1B, A2, B1 and scenario ensemble.

In the next section we first describe data and analysis technique. We then discuss the results in Section 3 and present our main conclusions in Section 4.

2 Data and Methodology

The CMIP3 dataset employed in the study is summarized in Table 1. It includes 14 models from laboratories worldwide spanning a horizontal resolution of about 1-4 degrees. It is noted that only 14 of the 23 CMIP3 models are selected in the analysis because they performed all the following simulations (see Table I): 20th century climate using observed GHG and aerosol forcing (referred to as 20C experiments), 21st century climate using GHG and aerosol forcing from the A1B, A2 and B1 emission scenarios of IPCC (1990). This set of scenarios spans almost the entire IPCC scenario range, with the B1 being close to the low end of the range (CO_2 concentration of about 550 ppm by 2100), the A2 to the high end of the range (CO_2 concentration of about 850 ppm by 2100) and the A1B to the middle of the range (CO_2 concentration of about 700 ppm by 2100). Some models include multiple realizations for the same experiment (Table 2.2), in which case only one realization is used in the analysis.

Monthly data for the CMIP3 experiments are obtained from the PCMDI web site (www.pcmdi-llnl.gov) and the reader is referred to this web site for more information about the participating models. Each CMIP3experiment consists of a control run (1901 – 1999) with constant (''present day'') atmospheric CO_2 and of a greenhouse run (2000 – 2099) with a standard gradual (1% yr21 compound) increase in CO_2. Because the models utilize different horizontal grids, for intercomparison purposes we interpolate the model data onto a common global 1 degree grid.. In addition, a common 1-degree land mask grid is defined, based on the half-degree grid of the observed dataset from the Climatic Research Unit (CRU) of the University of East Anglia (New

et al. 2000). This land mask grid is used as base for the calculations and, as a result, since the different models have different resolutions and thus different land configurations, this adds some uncertainty over coastal areas. However, this uncertainty is not large over the region of interest because the African coastline does not show very complex features.

The RCCI is calculated for 7 land regions of Africa from the latest set of climate change projections by 14 global climate models mentioned above for the A1B, A2 and B1 IPCC emission scenarios. Note that these scenarios almost encompass the entire IPCC scenario range, the A2 being close to the high end of the range, the B1 close to the low end and the A1B lying toward the middle of the range.

The RCCI is calculated for 7 land regions of Africa from the latest set of climate change projections by 14 global climate models mentioned above for the A1B, A2 and B1 IPCC emission scenarios.

Note that these scenarios almost encompass the entire IPCC scenario range, the A2 being close to the high end of the range, the B1 close to the low end and the A1B lying toward the middle of the range.

A Regional Climate Change Index (RCCI) is defined based on four variables: change in regional mean surface air temperature relative to the global average temperature change (or Regional Warming Amplification Factor, RWAF), change in mean regional precipitation (ΔP, % of present day value), change in regional surface air temperature interannual variability ($\Delta\sigma T$, % of present day value), change in regional precipitation interannual variability ($\Delta\sigma P$, % of present day value). In the definition of the RCCI it is important to include quantities other than the mean change because often mean changes are not the only important factors for determining impacts [e.g., Mearns et al., 2001]. We thus also include interannual variability, which is critical for many activity sectors, such as agriculture or water management. The RCCI is calculated for the above mentioned set of global climate change simulations and is intercompared across regions to identify climate change Hot-spots,that is regions with the largest values of RCCI.

Here ''change'' indicates the difference between the future 20-year climate periods of the 21st century and a present day climate period minimally affected by greenhouse gas (GHG) forcing (1960–1979).

As a measure of temperature interannual variability we use the interannual standard deviation ($\Delta\sigma T$) calculated for the selected 20-year periods. As a measure of precipitation variability we

use the coefficient of variation (i.e., the standard deviation divided by the mean, here denoted as $\Delta\sigma P$), which removes the dependency of the precipitation standard deviation on the mean. Both $\Delta\sigma T$ and $\Delta\sigma P$ are calculated after de-trending the data over the 20-year periods to obtain unbiased estimates of variability (Ra¨isa¨nen, 2002).

The RCCI is here defined as in Giorgi (2006), except that the entire yea is divided into two six months periods, MAMJJA and SONDJF.

$$RCCI=[n(\Delta P) + n(\Delta\sigma P)+n(RWAF)+n(\Delta\sigma T)]M..A+[n(\Delta P) + n(\Delta\sigma P)+n(RWAF)+n(\Delta\sigma T)]S.F$$

..(1)

As in Giorgi (2006) the integer n varies from 0 to 4 as described in Table 2.3 Note that small changes below a certain threshold do not contribute to the index (n=0) and that larger changes are weighted more heavily (i.e., the factor n doubles from each category to the next). As an illustrative example, if ΔP is the change (2081-2100 minus 1961-1980) in average precipitation for a given region, it is obtained via the follow steps: 1) Calculate ΔP for each individual region, averaging over each grid point in the region; 2) Average over the different models; 3) Average over the three scenarios (A1B, A2, B1). The same procedure is used to calculate grid point values (except for the regional averaging of course) and the values of RWAF, $\Delta\sigma T$ and $\Delta\sigma P$.

3 Results

Figure 1 shows the fine scale geographical distribution of the RCCI over Africa based on data compounded from each of the three scenarios A1B, A2, and B1 for the periods: 2081-2100, i.e. the period when the climate change signal is maximum, with respect to 1961-1980.

We find that the RCCI shows pronounced spatial variability over this region, varying from values less than 8 to greater than 16.

SMED and SAH have the largest RCCI value, where the contribution comes from the increase in precipitation interannual variability in MAMJJA and SONDJF seasons, decrease in mean precipitation in the two seasons, and small increase in the RWAF in MAMJJA. WAF, EAF, EQF have similar RCCI values and the contributions come from the increase in mean precipitation in the SONDJF season.

SAF RCCI value is relatively large and the contributions come from the decrease in the mean precipitation in the MAMJJA season, and small increase in the precipitation variability in the two seasons.

The contributions of the different components of the RCCI, in the period 2081-2100, for ensemble of the three scenarios (see Eq. 1) are shown in Figures 2. The contribution of precipitation generally shows complex patterns and substantial variability, especially for the interannual variability. For mean precipitation we can see symmetrical patterns around the equator which is consistent with the symmetry in the climatic zones in the northern and southern hemispheres in Africa. We find a large decrease in precipitation over the SMED in every sub-region, SAH in Egypt and Libya in MAMJJA and a small increase over the southern parts of Egypt, Libya and Algeria, but the value of the decrease exceeds that of the increase so when averaging over the SAH area, the decrease in precipitation is dominant in SONDJF case. Over SAF we find a large decrease in precipitation in the MAMJJA case. Over EQF, there is a small increase in the precipitation in MAMJJA and a large increase in SONDJF. Over WAF there is a small increase in precipitation in the SONDJF case. A large increase in precipitation is found over the EAF in the SONDJF season. In SQF an increase in precipitation over large parts in Tanzania and Congo balanced – to some extent- by decrease in precipitation.

The contribution of the changes in interannual variability shows complex patterns and marked geographical variations. As mentioned we mostly find an increase in variability, with noticeable exceptions occurring over parts in Mali and Niger in the WAF, North West of Sudan in EAF, and over Uganda in the EQF. The increase in variability is especially pronounced over SMED and SAH in the two seasons, while in SQF and SAF we find small increase in the precipitation variability. The marked spatial variability of the change in variability further highlights the need of a fine scale analysis of climate change variables.

The contribution of mean temperature change compared to global temperature change (RWAF) in both seasons shows a latitudinal gradient, with maximum values in the northern regions and decreasing values toward the equator, then increases again toward the south, with low values (< 1.1) around the coast line of Africa. This result is consistent with the basic latitudinal distribution of warming, which is generally maximum over high latitude and high elevation northern hemisphere regions due to the melting of

land and sea ice and the associated ice-albedo feedback mechanism, (Giorgi et al., 1997; Meehl et al. 2007 (CHAPTER10)), and also robust with the symmetry of climatic zones in the Northern Hemisphere as in the Southern Hemisphere, as they are arranged symmetrically on either side of the equator. The RWAF thus produces large contributions to the SMED, SAH and SAF regions. The contribution of changes in interannual temperature variability shows a more complex spatial distribution. In MAMJJA this contribution is especially large over the SAH in the north Egypt and north Libya, middle WAF and middle SQF. In SONDJF, the contribution of temperature variability change is maximum over the middle SQF. The west coast of Africa exhibits very small decrease in the temperature variability in the SONDJF season. Every region does not have large contribution from the temperature variability, which again sheds light on the need of not only the fine scale analysis of the climate variables but also a sub-region averaging of each of the seven regions.

In summary, the RCCI and the underlying changes that contribute to it, exhibit marked sub-regional variability that allows us to identify more hot-spots at spatial scales smaller than the sub-continental one used.

3.2. Dependency of the sub-regional hot-spots on the GHG forcing

The GHG forcing in the 21st century varies as a function of GHG emissions and concentrations, which in turn vary as a function of time and scenario (IPCC 2000). It is therefore important to investigate possible dependencies of the sub-regional hotspots on the GHG forcing. Figure 3 first shows the RCCI values averaged over each of the 7 regions of Africa calculated for 5 successive 20-year periods (2001-2020, 2021-2040, 2041-2060, 2061-2080, 2081-2100) with respect to 1961-1980 and for the mid-range A1B scenario, high-range A2 scenario, low-range B1scenario, and their average. In general, we find increasing values of RCCI with time, and thus with GHG forcing.

If for illustrative purposes we define an RCCI threshold of 10 to identify a hot-spot, the first to appear in 2021-2040 is SAH for A2, and having only a slightly smaller value for A1B and smaller in B1 scenario. The SMED and SAH hot-spots clearly emerge in 2041-2060 and remain well established (although with different temporal paths) with values greater than 10 for the rest of the century except for B1 scenario. The WAF and SQF hot-spots emerge in 2081-2100 for A2

scenario, the EAF and EQF hotspot emerges in 2061-2080 for A2 scenario and for A1B for SAF hotspot and maintain the largest RCCI values for the last decades of the century. The WAF, EAF, EQF and SQF show the least dependence on time (and GHG forcing). By the end of the century (2081-2100) SMED, SAH and SAF hot-spots identified are established except under B1 scenario, where the RCCI never exceeds 10, and consistent with those found by combining results from the three scenarios. The key message of Figure 3 is thus that different hot-spots emerge at different times of the 21st century (thus at different GHG forcing) and exhibit different temporal pathways throughout the 21st century.

For the period 2081-2100, figure 3 also compares the RCCI value under B1, A1B, A2 scenarios and their average, separately. Mostly the RCCI values increase with the GHG concentration and forcing, i.e. they are minimum in the B1 (low GHG) and maximum in the A1B and A2 (high GHG) scenarios except for EAF. Only the SMED and SAH hot-spots have RCCI values greater than 16, except for B1 scenario. The SMED and SAH hot-spots are the greatest in the A1B and A2 scenarios, but are not strong in the low GHG scenario B1. Finally, the EAF hot-spot show a different behavior from the rest, being greater in the B1 than the A1B scenarios. This implies that the dependency of the hot-spot on the forcing is not scenario-monotonic for all regions.

Also shown is the evolution of the values when all the scenarios are considered together (denoted as "ensemble", note that the RCCI for the ensemble is not the average RCCI of the three scenarios, but is calculated after averaging the climate change variables across the scenarios). Figure 3 illustrates well the different behavior across hot-spots. The RCCI for the SMED, SAH, and SAF regions (i.e. the northernmost and southernmost ones) increases almost linearly with time in the full ensemble average. However we also notice a decrease towards the end of the century for the SMED region in the B1 scenario, a decrease towards the end of the century for the SAH region in the A2 scenario, and a decrease towards the end of the century for the SMED and SAH regions in the A1B scenario.

For SMED, SAH, SQF, and SAF we see a monotonic increase of the RCCI, for scenario ensemble. The RCCI of the WAF and EQF regions flattening until the period 2021-2040, then increases monotonically. For the EAF region the RCCI increases until 2041-2060, followed by flattening until 2061-2080, then increases again toward the end of the century.

From figure 3 we can also compare the spread of the RCCI across scenarios with that across time slices. This spread can also be considered as a measure of uncertainty. The spread across time

slices dominates for all regions except for the SMED and SAH regions in the 2061-2080 and 2081-2100 periods, where the spread across scenarios dominates, while for the other hot-spots the dependency of the RCCI on time and scenario (and thus on GHG forcing) is relatively small, indicating a robust behavior of the hot-spot. In summary, Figure 3 is indicative of a rather complex spatial and temporal dependency of the sub-regional hot-spots on the GHG concentration (and forcing). This makes it difficult to linearly extrapolate the results of a RCCI analysis across regions, scenarios and time slices.

Finally the temporal evolution of the different contributions to the RCCI in the hot-spot regions is shown in Table 4 for scenario average. We again find markedly different behaviors across regions. The dominant contribution for the increase in RCCI value over the SMED and SAH regions is a mix of contributions from mean and variability changes in both seasons.

3.3. Summary and Conclusion

In this study we presented a fine scale analysis of the climate change signal over Africa from the CMIP3 ensemble based on the RCCI introduced by Giorgi (2006). It may be noted that RCCI is a comparative index and not an absolute one, i.e. it is designed to compare the climate change signal across regions but not to provide an absolute indication of the magnitude of the signal. This implies that small RCCI values are not necessarily an indication of a small magnitude of the change signal. Second, the RCCI combines information from different change indicators without weighting the importance of such indicators for local impacts. It is therefore possible that different variables used to define the RCCI might be more (or less) important for given impact applications. In addition, the choice of variables is somewhat subjective. For example, the RCCI does not include measures of extremes (although it might be expected that variability and extremes are somewhat related). Different choices of variables might lead to different measures of change and in fact Baettig et al. (2007) have proposed several change indices. In this regard, our preliminary tests show that in Giorgi's definition of RCCI, the choice of the values of the integer is not critical for the identification of sub-regional hot-spots.

The first major conclusion of our work is that, although as a whole Africa does not show a large RCCI compared to other regions of the world (i.e. it is not identified as a prominent climate change hot-spots, Giorgi 2006)), it still includes clearly identifiable sub-regions with high RCCI

values (i.e. sub-regional hot-spots). More specifically, we identify seven such hot-spots. This calls for a high resolution analysis to identify sub-regional hot-spots within broad sub-continental scale regions.

Our results also show that different hot-spots can exhibit markedly different response to GHG concentrations/forcings in terms of the timing of emergence and development of the hot-spot. In addition, the different contributions to the RCCI show complex temporal and cross-regional behavior.

These results point to the limitations of using linear scaling assumptions in this type of analysis, at least at the sub-regional scale identified here.

The identification of sub-regional hot-spots may provide important information for climate impact assessment studies and for designing priorities in terms of national and cross-national adaptation and mitigation policies. In this regard, the RCCI only provides an overall measure of climate response based on a limited number of variables and it is not aimed at specific impact studies. A RCCI-based analysis can be especially useful in providing insights on the behavior of regional climate changes in relation to globally averaged warming and as such it can provide a useful tool to identify sub-regions that are responsive and possibly vulnerable to climate change.

References

Baettig MB, Wild M, Imboden DM, 2007. A climate change index: Where climate change may be most prominent in the 21st century. *Geophysical Research letters*, **34**, L01705

Collins, M., and The CMIP Modelling Groups (2005), El Nin˜o- or La Nin˜alike climate change?, Clim. Dyn., 24, 89–104.

Giorgi, 2006: Climate change hot-spots. *Geophys. Res. Lett.,* **33,** L08707, doi:10.1029/2006GL025734.

Giorgi, F. (2005), Interdecadal variability of regional climate change: Implications for the development of regional climate change scenarios, Meteorol. Atmos. Phys., 89, 1 –15.

Giorgi, F., and X. Bi (2005a), Updated regional precipitation and temperature changes for the 21st century from ensembles of recent AOGCM simulations, Geophys. Res. Lett., 32, L21715, doi:10.1029/2005GL024288.

Giorgi, F., and X. Bi (2005b), Regional changes in surface climate interannual variability for the 21st century from ensembles of global model simulations, Geophys. Res. Lett., 32, L13701, doi:10.1029/

2005GL023002.

Giorgi, F., P. W. Whetton, R. G. Jones, J. H. Christensen, L. O. Mearns, B. Hewitson, H. vonStorch, R. Francisco, and C. Jack (2001), Emerging patterns of simulated regional climatic changes for the 21st century due to anthropogenic forcings, Geophys. Res. Lett., 28, 3317–3320.

Giorgi F, Francisco R (2000) On the predictability of regional climate change. Clim Dyn 16:169–182

Intergovernmental Panel on Climate Change (2000), Special Report on Emissions Scenarios, edited by N. Nakicenovic et al., 599 pp., Cambridge University Press, New York.

IPCC. 2007. Climate Change 2007: The Physical Science Basis. Contribution of WorkingGroup I to the Fourth Assessment Report of the Intergovernmental Panel on Climate Change. Solomon S, Qin D, Manning M, Chen Z, Marquis M, Averyt KB, Tignor M and Miller HL (eds). Cambridge University Press: Cambridge, United Kingdom and New York, NY, USA.

Meehl, G. A., and C. Tebaldi (2004), More intense, more frequent and longer lasting heat waves in the 21st century, Science, 305, 994– 997.

Mike Hulme, Ruth Doherty, Todd Ngara, Mark New, David Lister (2001): African Climate Change: 1900-2100, Clim Res, Vol. 17: 145–168, 2001.

Mitchell T, Hulme M (1999) Predicting regional climate change: living with uncertainty. Prog Phys Geogr 23: 57–78.

Ra¨isa¨nen, J. (2002), CO2-induced changes in interannual temperature and precipitation variability in 19 CMIP2 experiments, J. Clim., 15, 2395– 2411.

Santer BD, Taylor KE, Wigley TML, Johns TC, Jones PD, Karoly DJ, Mitchell JFB, Oort AH, Penner JE, Ramaswamy V, Schwarzkopf MD, Stouffer RJ, Tett S, Boyle JS, Parker DE (1996) Human effect on global climate. Nature 384: 523–524

Tables

Table 1 List of CMIP3 Models and Simulations Used in the Analysis

Models	Origin	Grid interval	Scenarios and ensemble members			
			20C	A1B	A2	B1
CCMA-3-T47	CCMA, Canadian	~2.7 deg	5	4	2	4
CNRM-CM3	CERFACS, France	~2.8 deg	1	1	1	1
CSIRO-MK3	CSIRO Atmos. Res., Australia	~2.3 deg	2	1	1	1
GFDL-CM2-0	Geophys. Fluid. Dyn. Lab., USA	~2.2 deg	3	1	1	1
GISS-ER	NASA Goddard Inst., USA	~4.5 deg	1	2	1	1
INMCM3	Insit. Numer. Math., Russia	~4.5 deg	1	1	1	1
IPSL-CM4	IPSL, France	~3.0 deg	1	1	1	1
MIROC3-2M	JAMSTEC, Japan	~2.8 deg	3	3	3	3
MIUB-ECHO-G	Germany/Korea	~3.2 deg	5	3	3	3
MPI-ECHAM5	MPI, Hamburg, Germany	~2.3 deg	3	2	3	3
MRI-CGCM2	MRI, Japan	~2.8 deg	5	5	5	5
NCAR-CCSM3	NCAR, USA	~1.4 deg	8	6	4	8
NCAR-PCM1	NCAR, USA	~2.8 deg	4	3	4	2
UKMO-HADCM3	UK Meteorological Office	~3.0 deg	1	1	1	1

Table 2 Values of the factor n in the definition of the RCCI.

n	ΔP	$\Delta\sigma_P$	RWAF	$\Delta\sigma_T$
0	<5%	<5%	<1.1	<5%
1	5-10%	5-10%	1.1-1.3	5-10%
2	10-15%	10-20%	1.3-1.5	10-15%
4	>15%	>20%	>1.5	>15%

Table 3 Definition of the seven regions in Africa over which the RCCI is studied.

Region		Longitude	Latitude
SMED	Southern Mediterranean	10.5 W - 37.5 E	30 N - 38 N
SAH	Sahara	19 W - 40.5 E	18 N – 30 N
WAF	Western Africa	19 W - 20.5 E	0 – 18 N

EAF	Eastern Africa	20.5 E – 52.5 E	0 – 18 N
EQF	Equatorial Africa	28.5 E – 43.5 E	8 S – 4 N
SQF	South Equatorial Africa	0.5 E – 55.5 E	26 S - 0
SAF	Southern Africa	9.5 E – 40.5 E	35 S – 26 S

Table 4 Values of ΔσT, RWAF, ΔσP, ΔP over the 7 regions in Africa. The corresponding value of n in equation (1) is shown in parentheses.

Sub-Reg-	Factors	2001-2020	2021-2040	2041-2060	2061-2080	2081-2100	2001-2020	2021-2040	2041-2060	2061-2080	2081-2100

ions		MAMJJA					SONDJF				
SMED	ΔP(%)	-0.75 (0)	-5.91 (1)	-13.65 (2)	-20.43 (4)	-24.33 (4)	-1.05 (0)	-5.37 (1)	-10.36 (2)	-16.03 (4)	-19.90 (4)
	ΔσP(%)	9.65 (1)	11.33 (2)	16.22 (2)	21.69 (2)	26.52 (4)	8.79 (1)	10.32 (2)	13.56 (2)	18.66 (2)	20.52 (4)
	RWAF	1.46 (4)	1.43 (2)	1.40 (2)	1.44 (2)	1.40 (2)	1.14 (1)	1.14 (1)	1.17 (1)	1.18 (1)	1.17 (1)
	ΔσT(%)	3.41 (0)	2.17 (0)	5.46 (1)	4.64 (0)	6.76 (1)	2.57 (0)	2.14 (0)	2.12 (0)	3.65 (0)	1.40 (0)
SAH	ΔP(%)	-0.10 (0)	-5.18 (1)	-12.43 (2)	-19.79 (4)	-23.57 (4)	-0.76 (0)	-5.11 (1)	-10.13 (2)	-15.73 (4)	-19.34 (4)
	ΔσP(%)	9.87 (1)	11.30 (2)	16.14 (2)	21.61 (4)	26.62 (4)	8.20 (1)	10.26 (2)	13.41 (2)	18.71 (2)	20.78 (4)
	RWAF	1.48 (2)	1.45 (2)	1.42 (2)	1.46 (2)	1.41 (2)	1.16 (1)	1.15 (1)	1.18 (1)	1.19 (1)	1.18 (1)
	ΔσT(%)	3.09 (0)	1.92 (0)	5.51 (1)	4.23 (0)	6.05 (1)	3.04 (0)	2.59 (0)	2.51 (0)	3.70 (0)	1.91 (0)
WAF	ΔP(%)	0.53 (0)	-0.86 (0)	-2.65 (0)	-2.26 (0)	-4.95 (0)	7.80 (1)	7.36 (1)	9.30 (1)	9.63 (1)	10.55 (2)
	ΔσP(%)	3.71 (0)	4.14 (0)	6.55 (1)	7.82 (1)	9.50 (1)	4.46 (0)	3.79 (0)	3.19 (0)	3.70 (0)	5.55 (1)
	RWAF	1.21 (1)	1.24 (1)	1.24 (1)	1.26 (1)	1.26 (1)	1.19 (1)	1.19 (1)	1.21 (1)	1.22 (1)	1.23 (1)
	ΔσT(%)	1.78 (0)	3.23 (0)	4.84 (0)	5.73 (1)	8.16 (1)	3.28 (0)	2.64 (0)	4.99 (0)	3.69 (0)	5.15 (1)
EAF	ΔP(%)	2.58 (0)	0.09 (0)	0.23 (0)	0.71 (0)	0.67 (0)	8.65 (1)	12.67 (2)	15.63 (4)	21.90 (4)	25.93 (4)
	ΔσP(%)	3.63 (0)	6.11 (1)	7.15 (1)	7.03 (1)	7.52 (1)	4.21 (0)	4.30 (1)	2.20 (0)	1.40 (0)	3.34 (0)
	RWAF	1.15 (1)	1.20 (1)	1.20 (1)	1.22 (1)	1.23 (1)	1.21 (1)	1.18 (1)	1.19 (1)	1.20 (1)	1.20 (1)
	ΔσT(%)	4.10 (0)	5.00 (1)	7.66 (1)	8.88 (1)	8.64 (1)	3.07 (0)	2.33 (0)	3.63 (0)	4.22 (0)	5.24 (1)
EQF	ΔP(%)	2.92 (0)	4.15 (0)	3.04 (0)	8.77 (1)	10.45 (2)	5.52 (1)	8.23 (1)	10.60 (2)	16.29 (4)	20.95 (4)
	ΔσP(%)	2.94 (0)	3.93 (0)	1.52 (0)	3.24 (0)	3.08 (0)	5.30 (1)	3.17 (0)	1.96 (0)	0.52 (0)	0.30 (0)
	RWAF	1.06 (0)	1.10 (1)	1.11 (1)	1.11 (1)	1.12 (1)	1.10 (1)	1.08 (0)	1.07 (0)	1.09 (0)	1.09 (0)
	ΔσT(%)	4.70 (0)	5.24 (1)	6.45 (1)	7.20 (1)	7.88 (1)	0.42 (0)	-0.61 (0)	2.09 (0)	3.18 (0)	3.32 (0)
SQF	ΔP(%)	0.14 (0)	-1.96 (0)	-3.61 (0)	-4.25 (0)	-4.25 (0)	-0.77 (0)	-1.75 (0)	-3.40 (0)	-4.21 (0)	-3.58 (0)
	ΔσP(%)	4.63 (0)	6.23 (1)	7.02 (1)	10.40 (2)	12.21 (2)	6.80 (1)	7.15 (1)	8.29 (1)	9.71 (1)	13.17 (2)
	RWAF	1.21 (1)	1.20 (1)	1.19 (1)	1.22 (1)	1.23 (1)	1.21 (1)	1.20 (1)	1.19 (1)	1.23 (1)	1.23 (1)
	ΔσT(%)	4.84 (0)	5.69 (1)	9.02 (1)	9.02 (1)	11.83 (2)	3.17 (0)	3.36 (0)	6.64 (1)	7.05 (1)	8.19 (1)
SAF	ΔP(%)	-5.40 (1)	-8.05 (1)	-10.97 (2)	-14.49 (2)	-15.59 (4)	-1.49 (0)	-4.24 (0)	-6.17 (1)	-7.79 (1)	-7.36 (1)
	ΔσP(%)	4.42 (0)	6.25 (1)	7.59 (1)	8.67 (1)	14.19 (2)	4.21 (0)	4.84 (0)	7.06 (1)	10.10 (2)	10.95 (2)
	RWAF	1.14 (1)	1.17 (1)	1.16 (1)	1.22 (1)	1.22 (1)	1.20 (1)	1.21 (1)	1.22 (1)	1.25 (1)	1.23 (1)
	ΔσT(%)	1.05 (0)	3.84 (0)	2.13 (0)	3.76 (0)	6.46 (1)	2.42 (0)	-0.33 (0)	-2.08 (0)	-0.35 (0)	1.31 (0)

Figures

Figure 1 Hotspots over Africa, for the period 2081-2100, A1B, A2 and B1 Scenario Ensemble
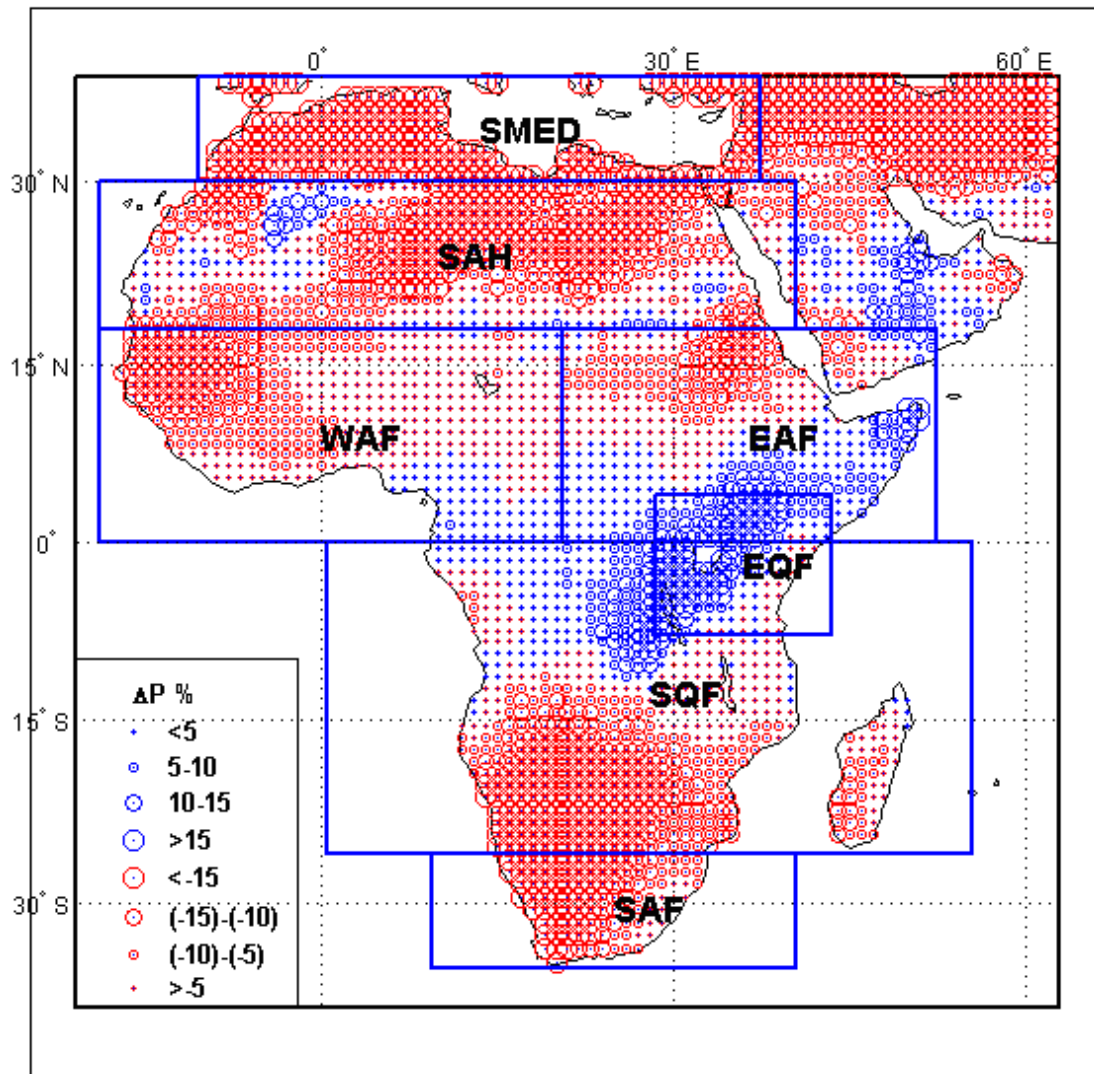
Figure 2 (a.1) Contribution of ΔP in MAMJJA season.
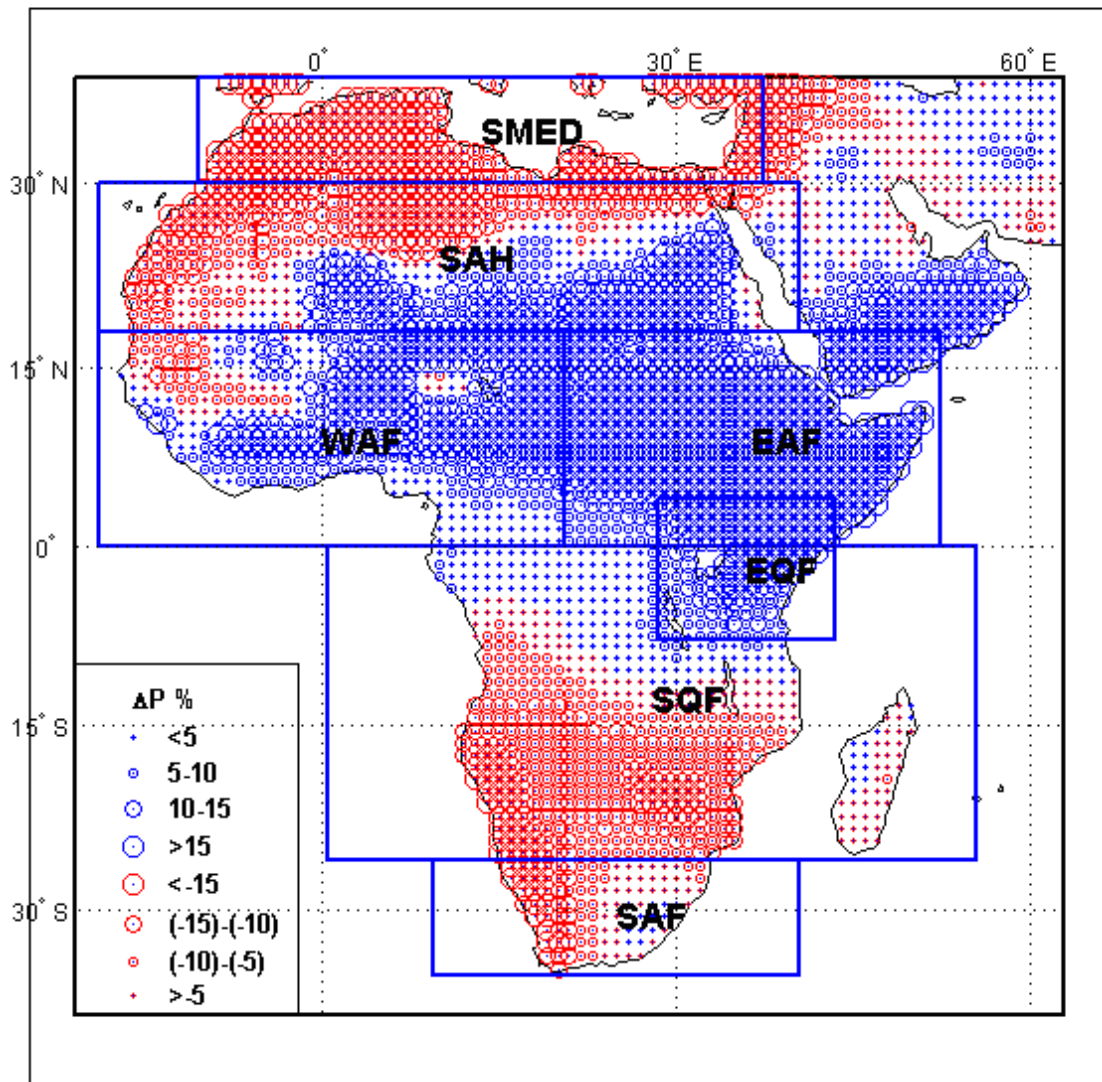
Figure 2 (a.2) Contribution of ΔP in SONDJF season.
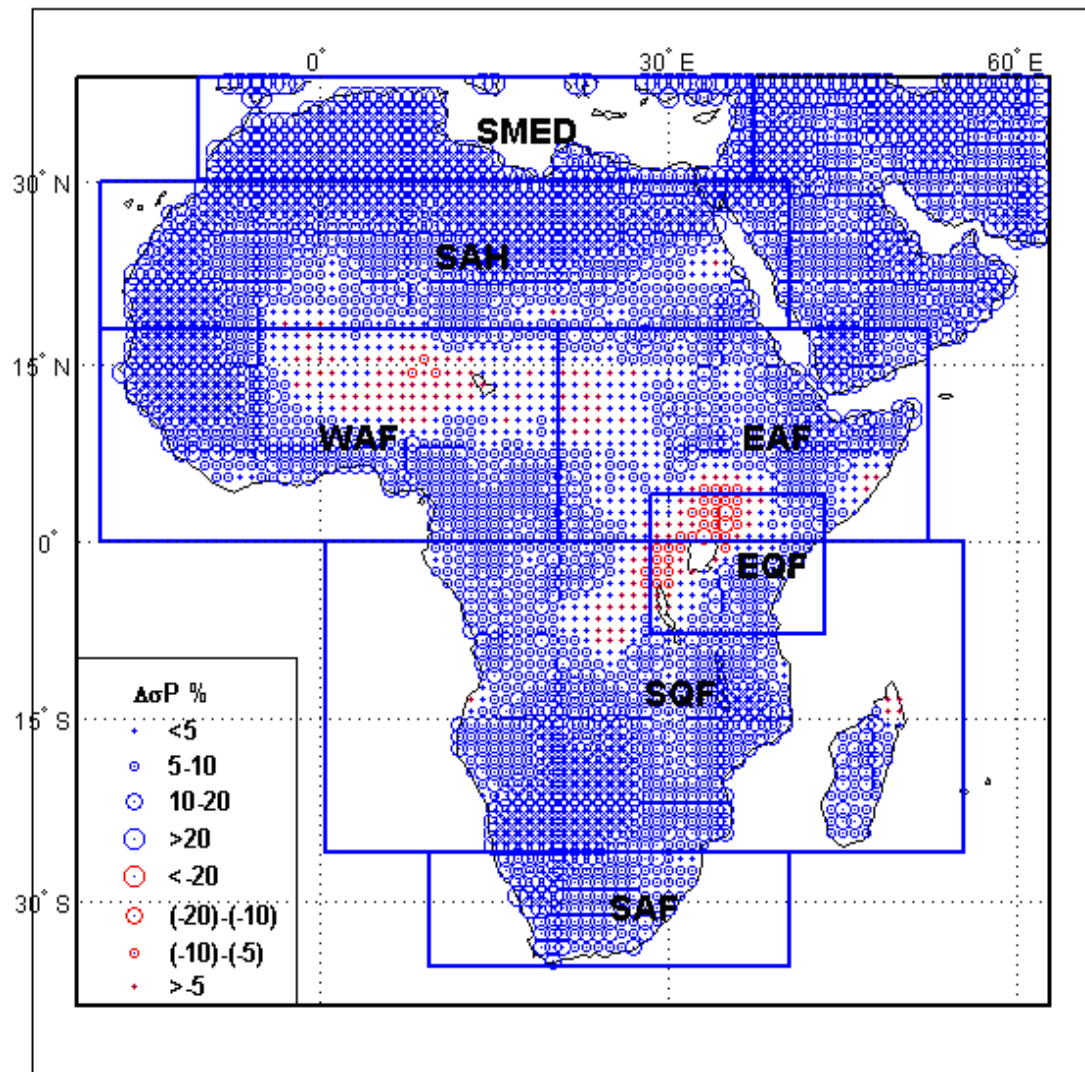
Figure 2 (b.1) Contribution of ΔσP in MAMJJA season.
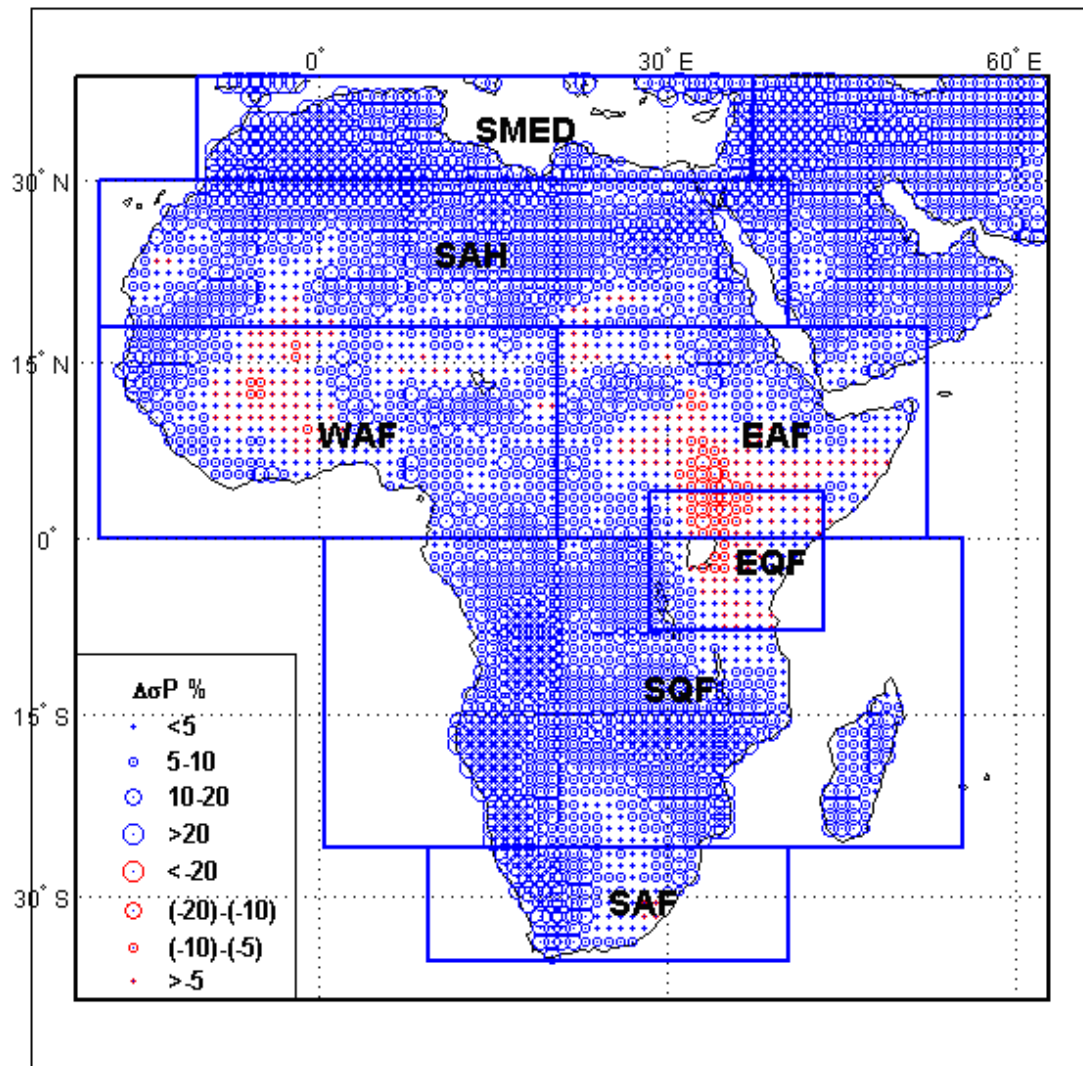
Figure 2 (b.2) Contribution of ΔσP in SONDJF season.
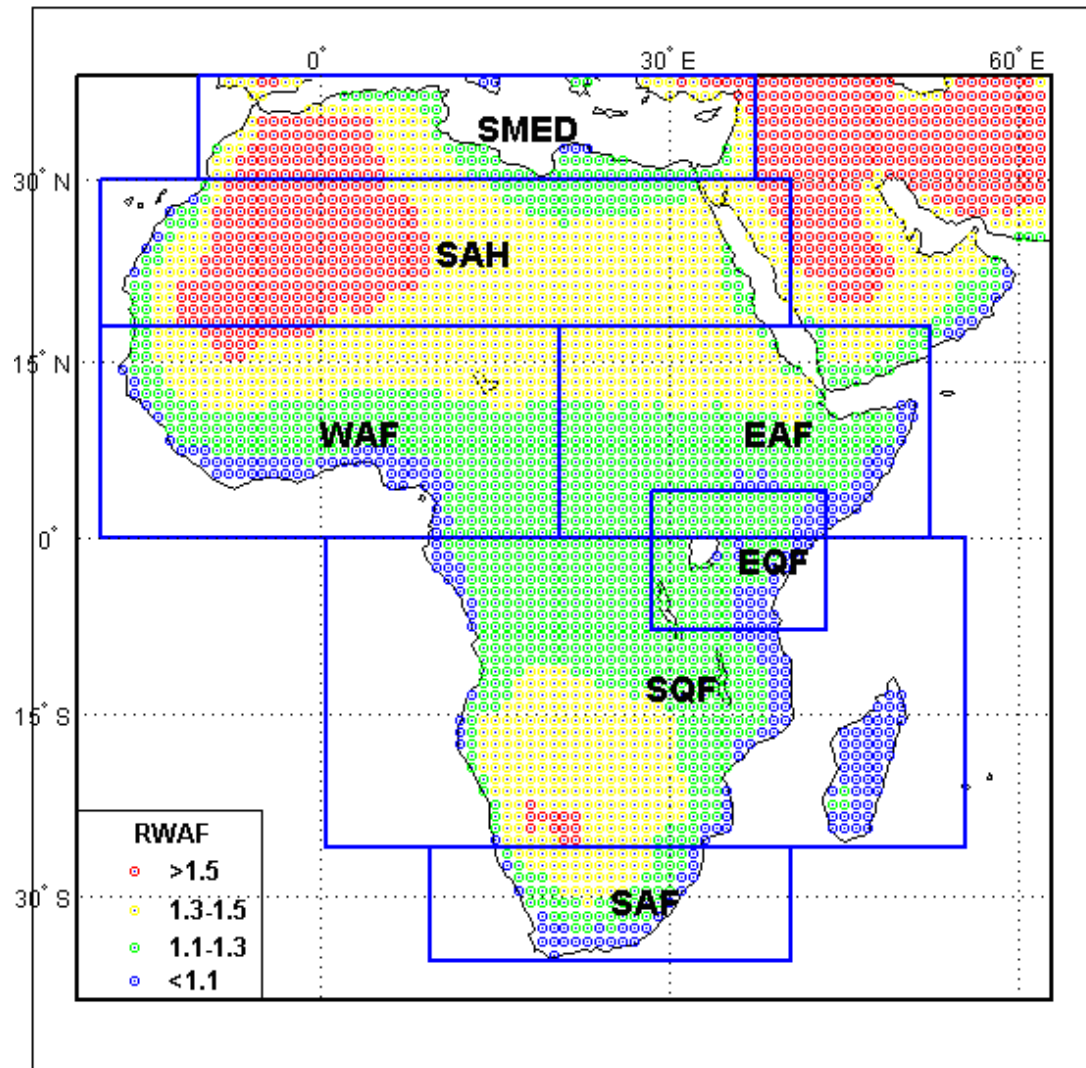
Figure 2 (c.1) Contribution of RWAF in MAMJJA season.
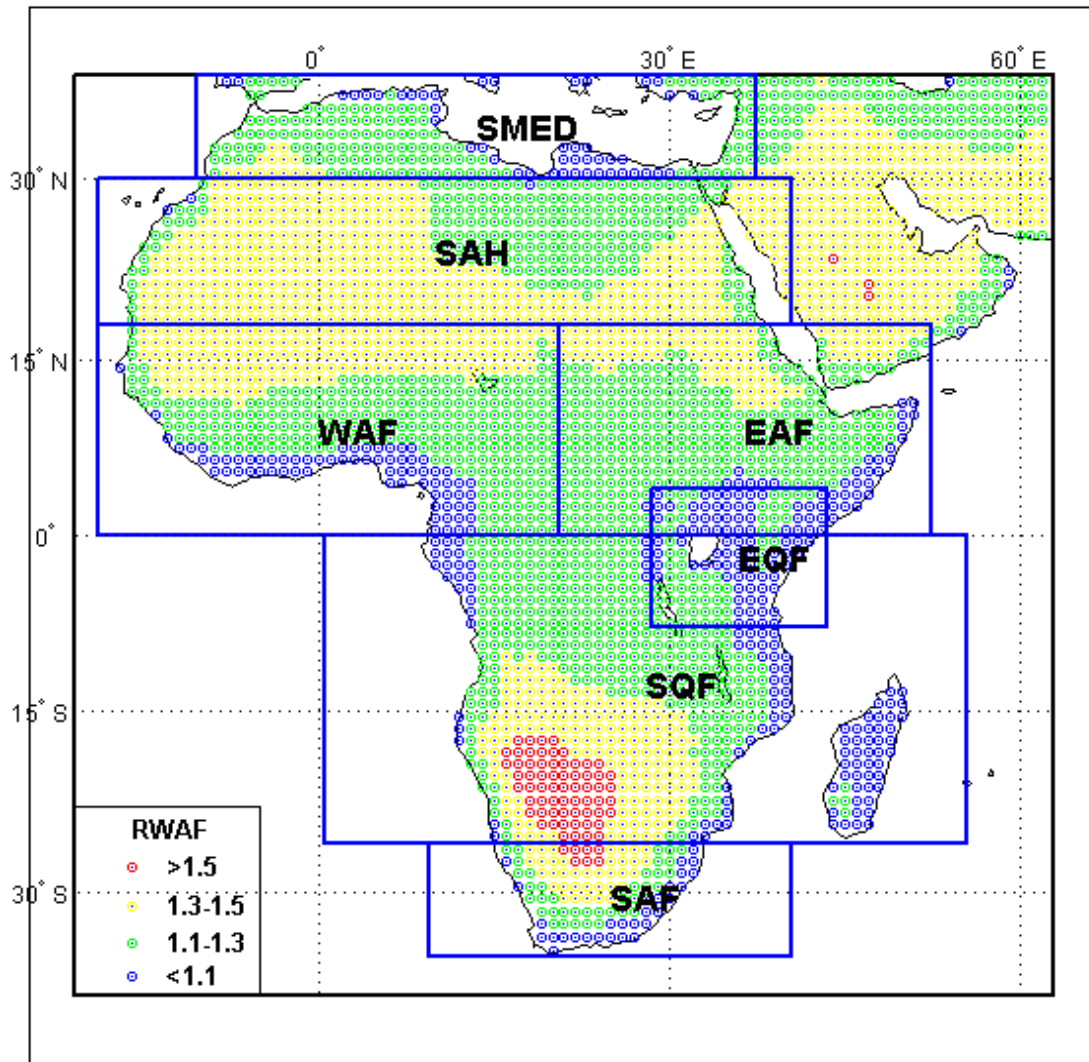
Figure 2 (c.2) Contribution of RWAF in SONDJF season.
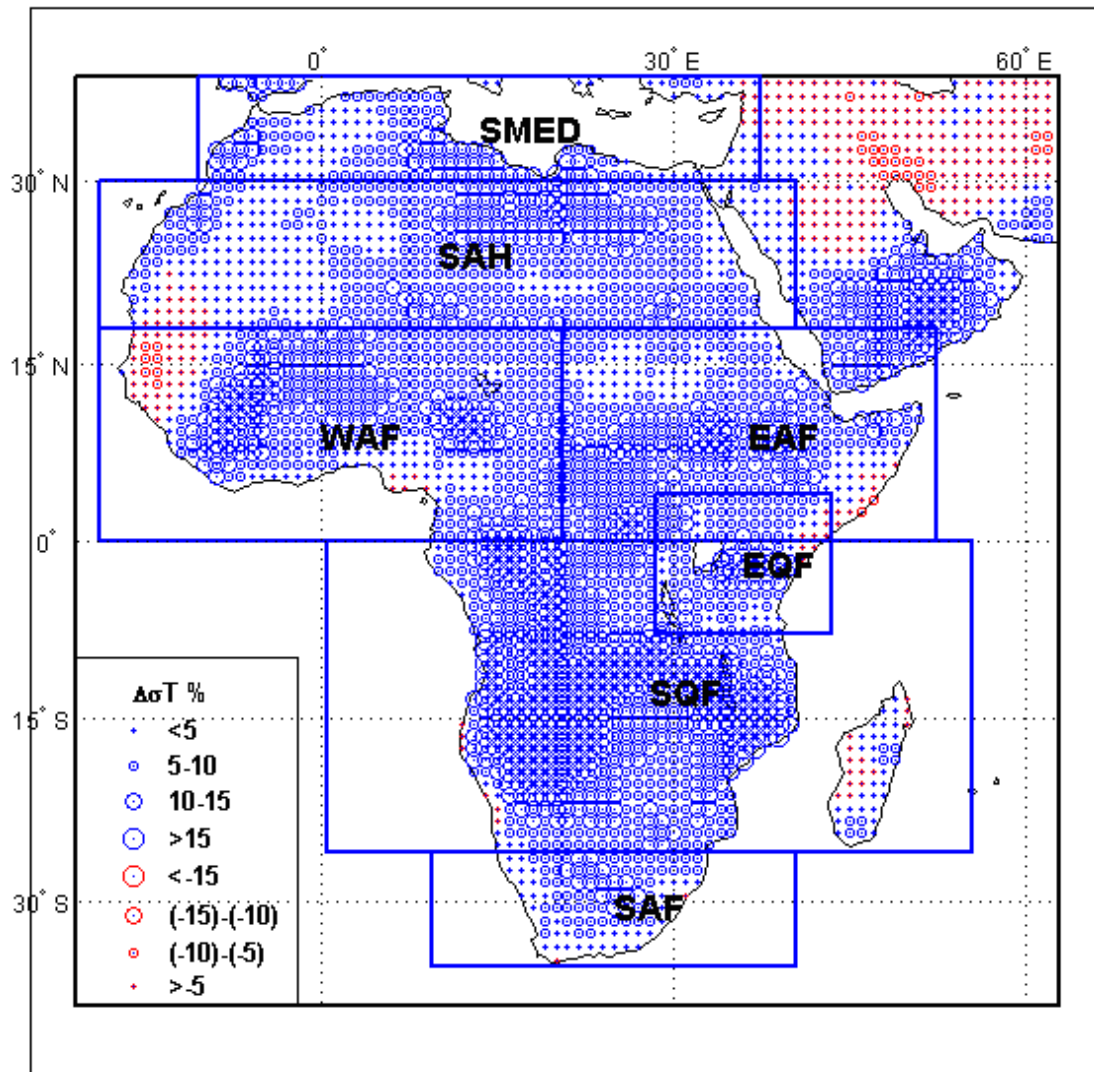
Figure 2 (d.1) Contribution of ΔσT in MAMJJA season.
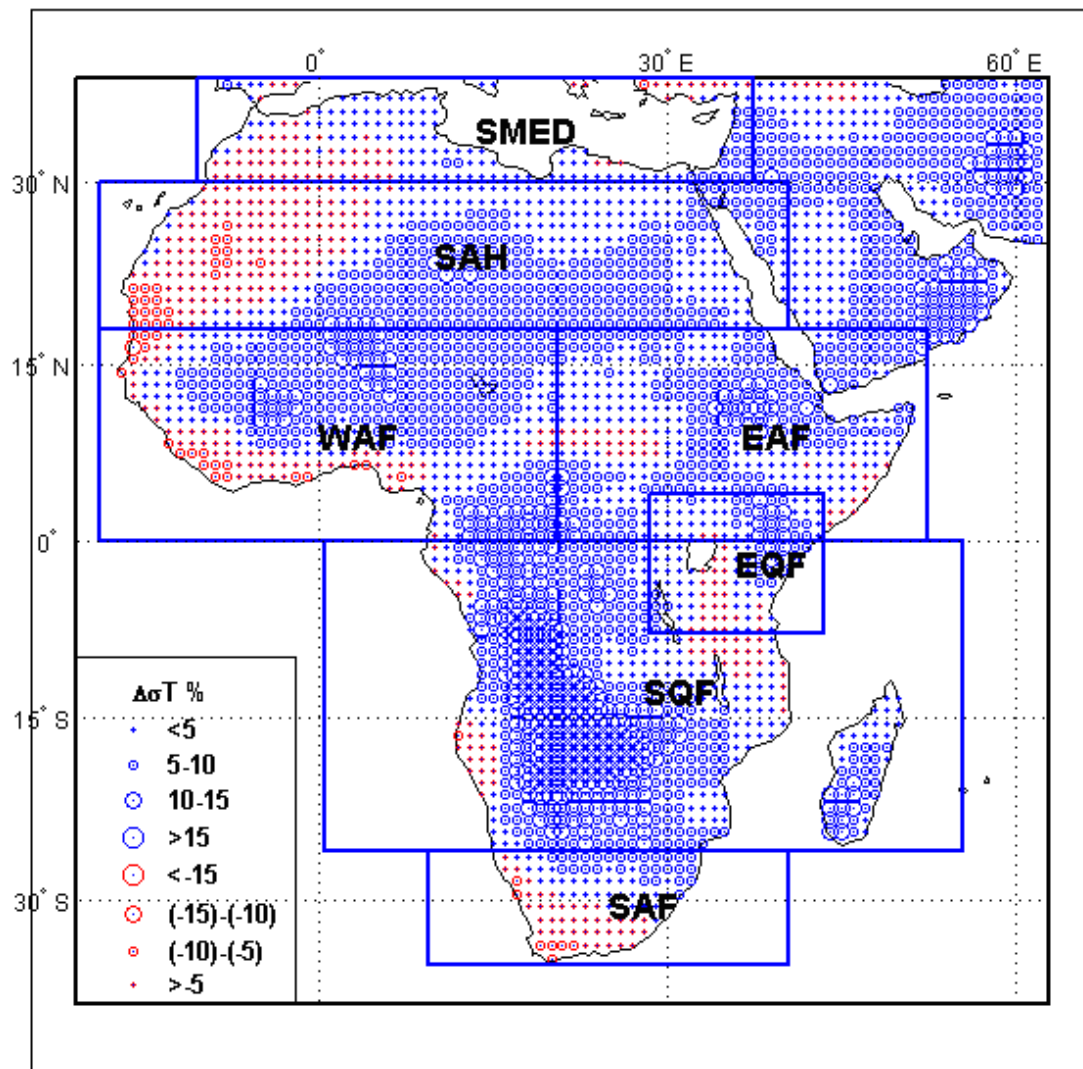
Figure 2 (d.2) Contribution of ΔσT in SONDJF season.
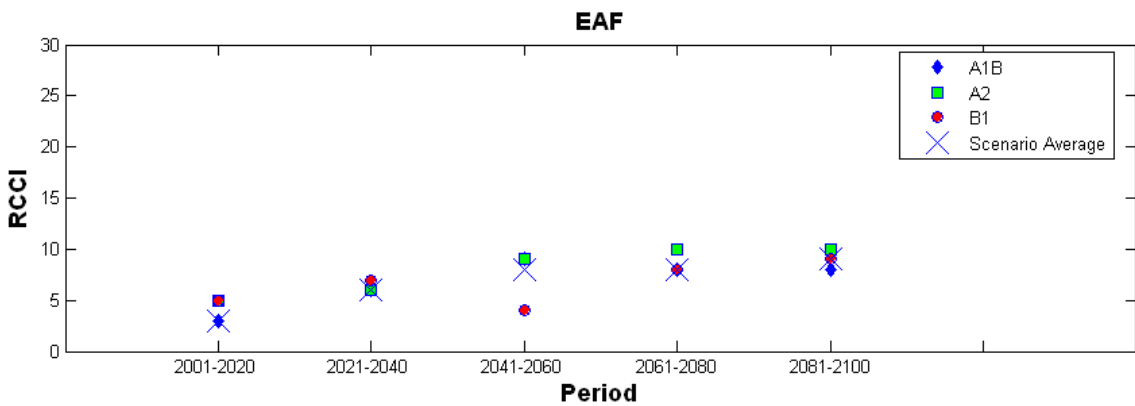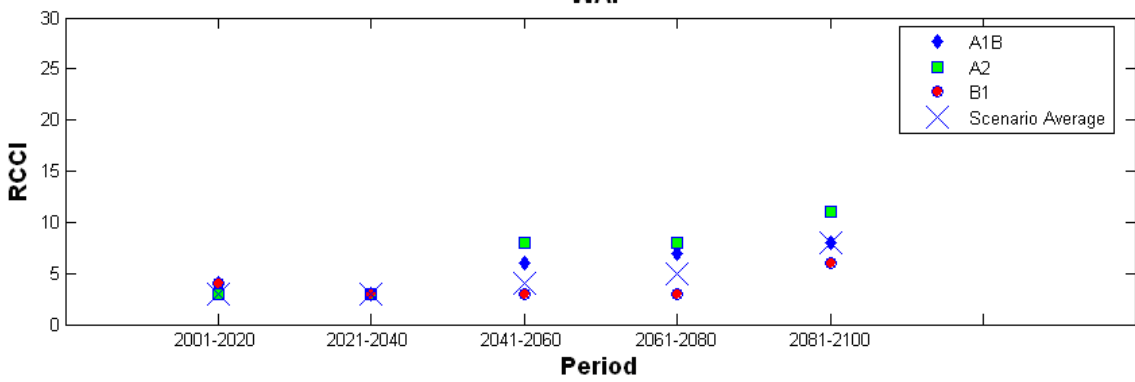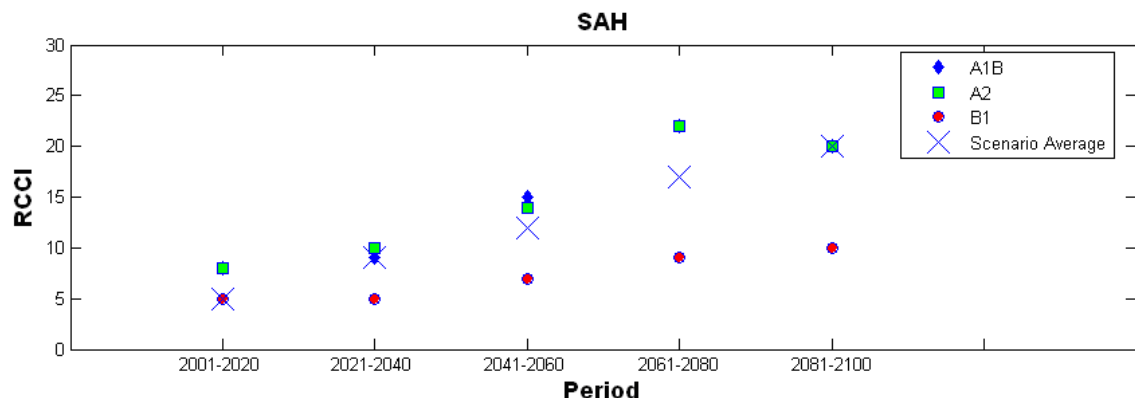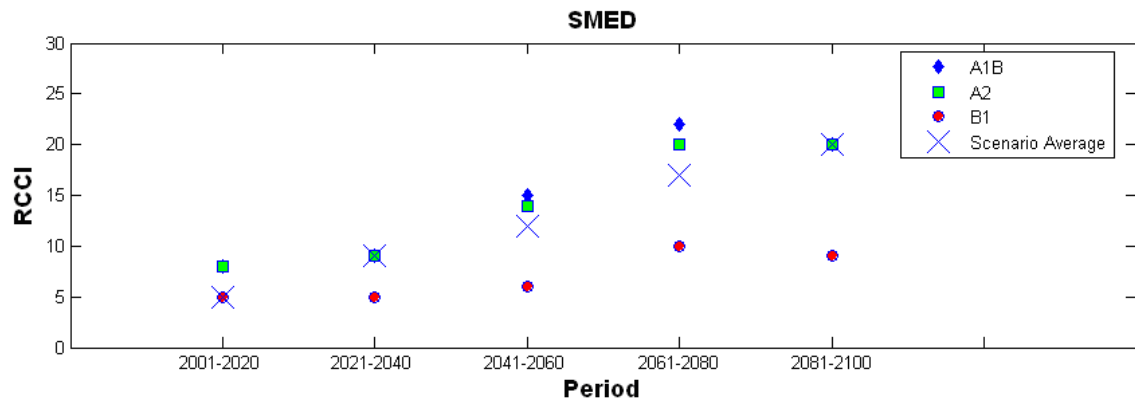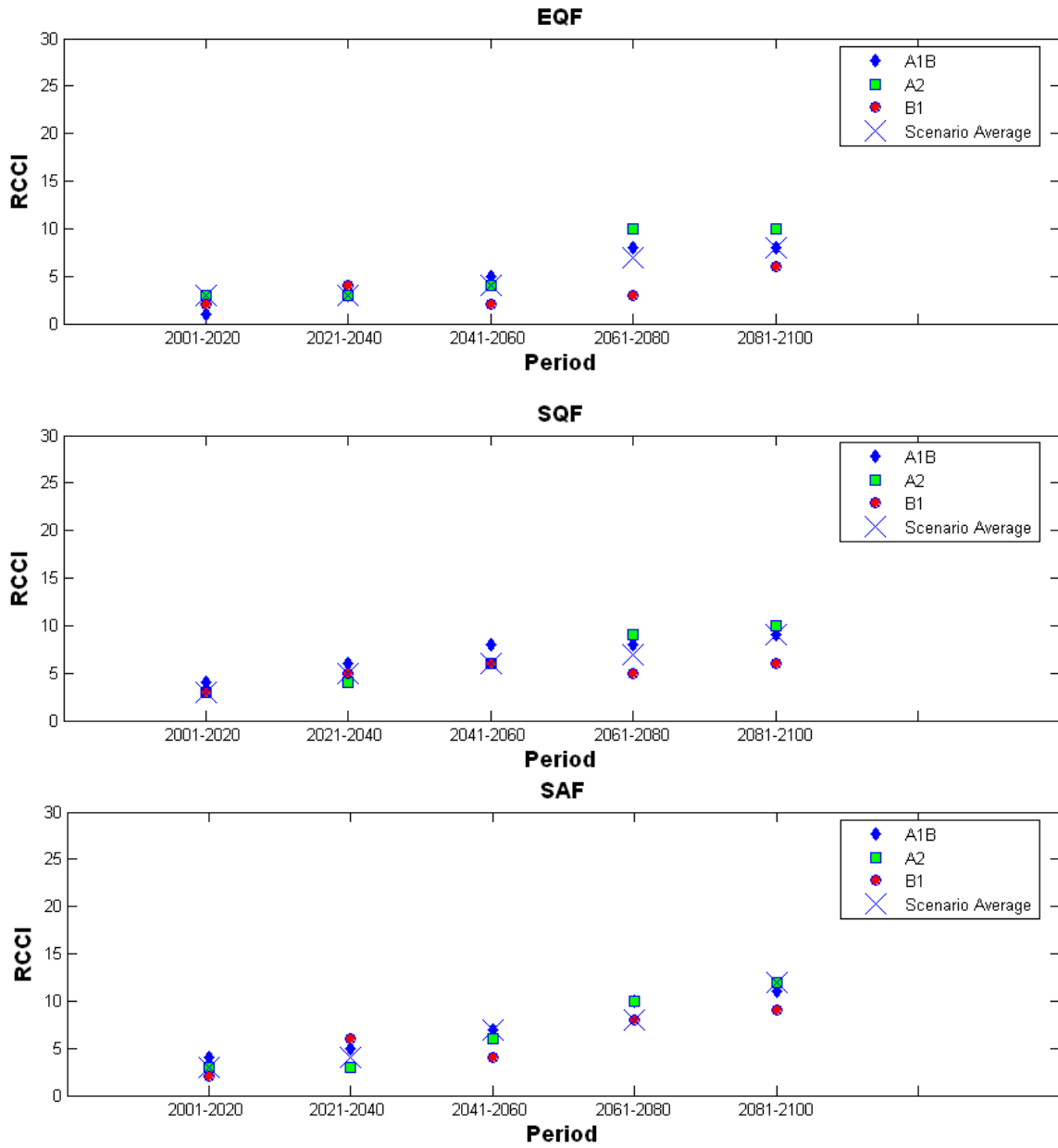
Figure 3 Variation of the RCCI with the five 20-year periods of the 21st century

for A1B, A2, B1 and scenario ensemble, for 7 regions in Africa.